

## Sintering behavior of 3 mol% yttria-stabilized CAD/CAM dental zirconia with different types of commercial powder

Yong-In Kim<sup>a</sup>, Si-Hwa Sung<sup>a</sup>, Seung-Mi Lee<sup>a</sup>, Wonsik Lee<sup>b</sup>, Sang-Hyeok Lee<sup>c</sup>, Bum-Sun Lim<sup>c</sup>, Ju-Suk Byun<sup>d</sup>, Chang-Yong Hyun<sup>a</sup>, Yeon Hwang<sup>a</sup> and Jai-Won Byeon<sup>a,\*</sup>

<sup>a</sup>Department of Materials Science and Engineering, Seoul National University of Science and Technology, Seoul 139-743, Korea

<sup>b</sup>Advanced Fusion Process R&D Group, Korea Institute of Industrial Technology, Incheon Metropolitan City, 406-840, Korea

<sup>c</sup>Department of Dental Biomaterials Science, College of Dentistry, Seoul National University, Seoul, Korea

<sup>d</sup>Gangnam Technology Appraisal Center, Korea Technology Finance Corporation, Seoul 135-080, Korea

Hybrid manufacturing converging cold isostatic pressing, ceramic sintering, and CAD/CAM process has been recently introduced for complex dental restoration instead of conventional wax casting. In this work, sintering behavior of 3% yttria-stabilized tetragonal zirconia polycrystal (3Y-TZP) was comparatively studied using three types of commercial spray-dried nano-powder. Cold isostatic pressed powders were sintered at 1250 °C ~1450 °C for 2 hours in order to fabricate fully sintered dental block of very fine tetragonal grain structure and high strength. Structural evolutions including relative density, shrinkage rate, grain growth, and fraction of monoclinic phase were investigated with sintering temperature. The observed sintering behaviors were discussed in relation with the characteristics of starting materials such as property of spray-dried granule as well as powder size and morphology. The fracture toughness of sintered blocks was in the range of 5.2~6.7 MPa.m<sup>1/2</sup>. Furthermore, for statistical analysis of the flexural strength based on failure probability, the shape and scale factor were determined from Weibull regression plot using 30 strength data for each type of powder. The sintered block of polygonal-shaped spray-dried nano-powders shows the highest shape factor and scale factor, implying that it is the most reliable and predictable in terms of fracture strength of sintered dental 3Y-TZP block.

**Key words:** 3Y-TZP, Dental zirconia, Cold isostatic press, Sintering, Weibull analysis.

### Introduction

Zirconia has three polymorphs of monoclinic, tetragonal and cubic phase. The tetragonal phase of zirconia can be stabilized at room temperature by doping with oxides such as Y<sub>2</sub>O<sub>3</sub>, CaO, MgO, and CeO<sub>2</sub>. Particularly, 3 mol% yttria-stabilized tetragonal zirconia polycrystal (3Y-TZP) ceramic has been being developed for mechanical engineering parts and dental restorations because of its high fracture toughness, fracture strength, and biocompatibility [1].

Hybrid manufacturing technology for fabrication of personally-fitting dental restorations is growing rapidly. This hybrid process involves powder pressing, ceramic sintering, and CAD/CAM process instead of conventional impressing, wax-molding, casting, and machining.

Inherently, 3Y-TZP ceramic is very difficult to machine for obtaining complex shape of dental parts due to high strength and brittle nature. Therefore, as a recently-growing hybrid fabrication process for dental parts applying CAD/CAM technique, soft porous preform of 3Y-TZP can be machined and then sintered for final

products. For this hybrid manufacturing process, optimum porosity level of preform is important for easy machining, and shrinkage rate is also important for compensation of dimension of final product.

In general, a fine microstructure of full density is required for engineering ceramics to achieve good mechanical properties, which can be achieved by optimum sintering process using nano-sized powder. 3Y-TZP is even more sensitive to grain size in relation with the stress induced tetragonal-to-monoclinic transformation that is a particular toughening mechanism of 3Y-TZP [1, 2].

On the other hand, final microstructure and mechanical property of the 3Y-TZP depends strongly on the characteristics of the starting materials such as granule property, size and morphology of powder, monoclinic/tetragonal phase fraction [1-4].

Improvement of mechanical properties can be achieved by optimizing sintering process in terms of micro-pore, grain growth, and crystalline phase. In this study, in order to fabricate a fully sintered 3Y-TZP block with very fine tetragonal grain, high fracture strength, and high reliability, three types of commercial 3Y-TZP powders with different powder characteristics were used. Sintering behavior and mechanical properties were compared among the specimens fabricated using these powders.

\*Corresponding author:

Tel : +82-2-970-6634

Fax: +82-2-973-6657

E-mail: byeonjw@seoultech.ac.kr

## Experimental Procedure

Three different types of commercial 3 mol% yttria-stabilized zirconia powders produced for biomedical and dental applications (3Y-TZP) were used as starting materials and their chemical compositions are summarized in Table 1. The chemical compositions are almost same among the 3Y-TZP powders supplied from different company. Table 2 show physical characteristics of the powders, including granule size, weight fraction of monoclinic zirconia phase, amount of binder, powder size and morphology. These powder characteristics would affect subsequent sintering behaviors. A-type powders contain larger amount (46 wt%) of monoclinic-ZrO<sub>2</sub> phase compared with B and C-type powders of relatively small amount (23 wt%). Average particle sizes of all powders are under 100 nm. The morphology of A and B-type powder was sphere, whereas C-type powders contain partially a polygonal morphology as described by the supplier.

The porous preforms of three different powders were produced by a cold isostatic pressing (CIP) with the pressure range of 200–350 MPa after uniaxial pressing of 10 MPa in a tungsten mold with a diameter of 19 mm. The specimens were sintered at sintering temperature range of 1250 °C–1450 °C with a heating rate of 5 °C/min for 2 hours in air.

Relative density of sintered specimen was measured by Archimedes' method. The weight fraction of the monoclinic zirconia phase was evaluated by using X-ray diffraction (XRD) peaks obtained in the 2θ range of 20 to 40 degree with a step width of 0.02° [4]. The microstructure was observed by a scanning electron microscope (SEM) after thermal etching at 1250 °C.

Fracture toughness,  $K_{IC}$ , was determined using the

indentation method. For each specimen, 10 indentation imprints were obtained under a load of 10 kgf. The fracture toughness was calculated using the following equation [5].

$$K_{IC} = 0.016 \times \left( \frac{E}{H} \right)^{0.5} \times \left( \frac{P}{C^{1.5}} \right) \quad (1)$$

Where,  $K_{IC}$ ,  $E$ ,  $H$ ,  $P$ , and  $C$  is fracture toughness (MPa m<sup>1/2</sup>), Young's modulus (GPa), Vickers hardness (GPa), applied force (N), and crack length (m), respectively.

Biaxial flexural strength was measured by a piston-on-3ball method as described ISO standard 6872 for dental ceramics. Disk-shaped specimens with a diameter of 15 mm and thickness of 1.3±0.2 mm were prepared for the test.

For statistical analysis of 30 flexural strength data obtained from each type of specimen, Weibull regression analysis was carried out to obtain shape factor (i.e., Weibull modulus) and scale factor (i.e., probabilistic fracture strength) for assessing fracture reliability of the sintered 3Y-TZP block. The description of the Weibull distribution function is given by the formula [6].

$$P(f) = 1 - \exp \left[ -V \left( \frac{\sigma}{\sigma_0} \right)^m \right] \quad (2)$$

Where,  $P(f)$ ,  $V$ ,  $\sigma$ ,  $\sigma_0$ , and  $m$  represent a fracture probability, specimen volume, fracture strength, the characteristic strength at the fracture probability of 63.21% and Weibull modulus, respectively.

## Results and Discussion

Fig. 1 is a scanning electron micrograph showing the morphology of powder granules (a, b, c) and individual powder in the granule (d, e, f) of the as-received materials. Comparing with sphere shape of A and B-type powders, polygonal shape of C-type powder was found. A-type granule appears to be denser than B and C-type granules. This image implies that each powder in A-type granule was strongly agglomerated each other.

**Table 1.** Chemical composition of three types of commercial 3Y-TZP powder. [wt%]

Type of powder	ZrO <sub>2</sub>	Y <sub>2</sub> O <sub>3</sub>	Al <sub>2</sub> O <sub>3</sub>	SiO <sub>2</sub>	FeO <sub>3</sub>	Na <sub>2</sub> O
A	94.1	5.1	0.250	0.003	0.005	-
B	94.5	5.2	0.236	0.002	0.002	0.019
C	94.4	5.3	0.248	0.002	0.002	0.013

**Table 2.** Physical properties of the spray-dried 3Y-TZP powder used for this research.

Type of powder	Granule		Powder				
	Size <sup>1</sup> [μm]	Fluidity <sup>2</sup> [g/sec]	Fraction of Monoclinic <sup>3</sup> [wt%]	Binder* [wt%]	BET Surface Area* [m <sup>2</sup> /g]	Size* [nm]	Shape*
A	33	0.78	46	3.2	16±2	37	Sphere
B	41	0.64	23	3.0	16±3	27	Sphere
C	54	0.64	23	3.0	7±2	90	Polygonal

\*: Data from supplier

1: Measured from SEM micrograph (Fig. 1)

2: Measured by powder fluidity tester

3: Determined from XRD result (Fig. 8)

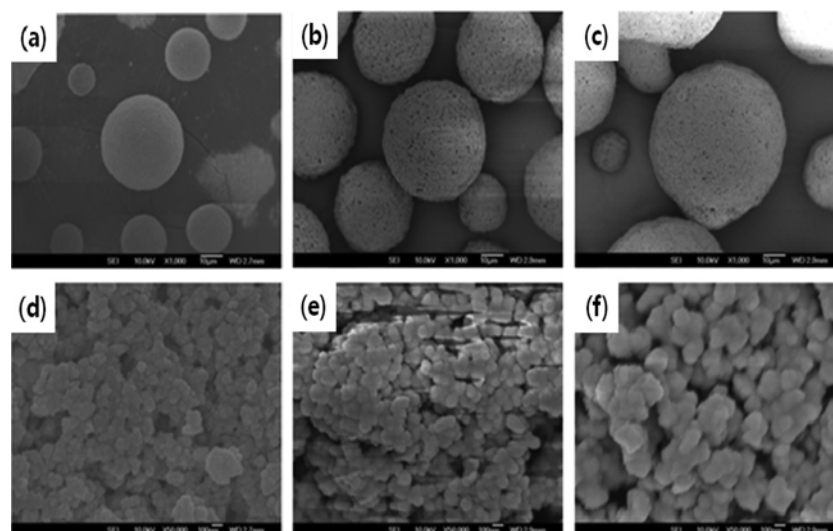


**Fig. 1.** SEM images of the spray-dried granule and powders in the granule; (a) granule-A type, (b) granule-B type, (c) granule-C type, (d) powder-A type (sphere), (e) powder-B type (sphere), (f) powder-C type (polygonal).

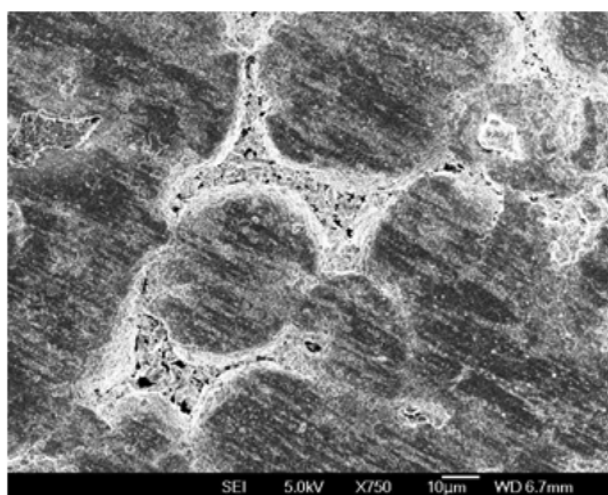


**Fig. 2.** SEM image of A-type compacted specimen under the uniaxial pressure of 150 MPa, showing insufficient compacting between each granule.

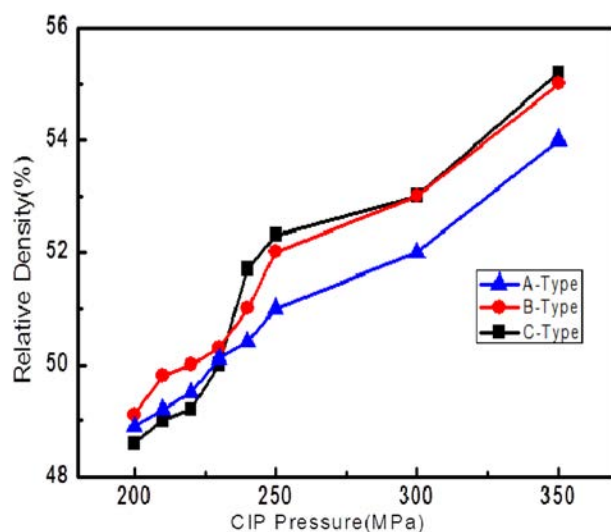


**Fig. 3.** Change of relative density of CIPed preforms with cold isostatic pressure

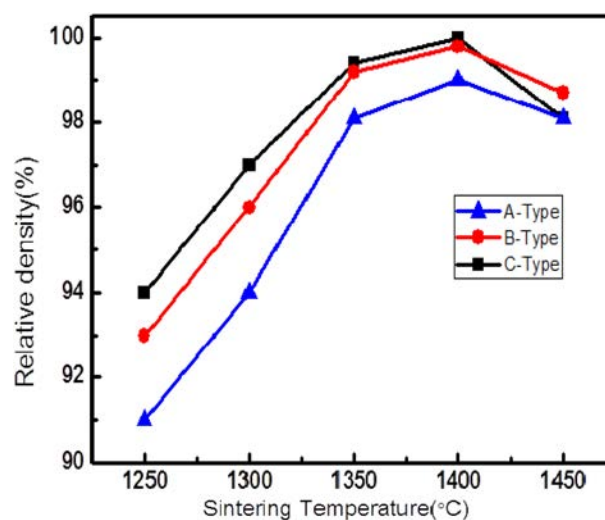


**Fig. 4.** Change of relative density with sintering temperature of the CIPed compacts prepared from three different types of powder.

Fig. 2 are SEM images of the compacted specimen under the uniaxial pressure of 150 MPa, showing the green compressibility of each type of powder. A-type granule reveals an insufficient breakage, implying low compressibility.

Fig. 3 shows relative density of CIPed porous preforms. Due to the difficulty of machining of brittle ceramic dental block, porous preform of 3Y-TZP block are needed for CAD/CAM machining before final sintering for the actual products. For easy machining, the strength of dental part applying CAD/CAM machining process should be neither too soft nor too hard. The fabricated preforms are recommended to have optimum relative density of 40~60% [7, 8]. In our work, the porous blocks with about 52% of relative density were obtained at the CIP pressure of 250 MPa, as shown in Fig. 3.

Fig. 4 shows the relative density of the CIPed

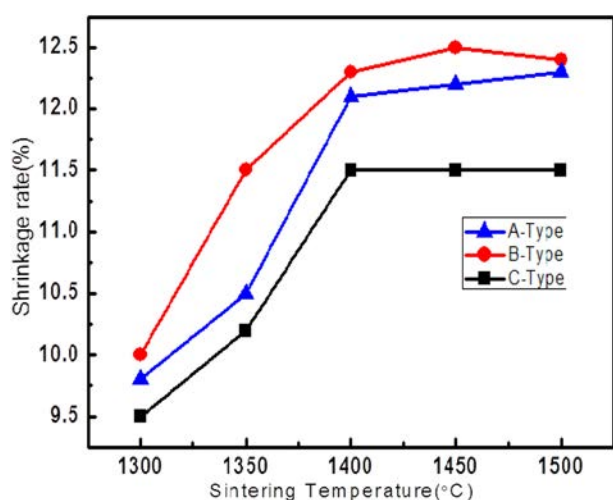


**Fig. 5.** Shrinkage rate of the CIPed compacts with sintering temperature.

compacts with sintering temperature. For all types of powder, the density increased up to 1400 °C before slight decrease at 1450 °C. Despite the slight difference among types of powder, the relative density of all types of powders reached about 98% at sintering temperature of 1350 °C. The sintering rate was in the order of type C>B>A. The latest sintering behavior of A-type powder can be attributed to bad compressibility of the A-type granule as shown in Fig. 2. Comparing B-type with C-type powder in the view point of the general

relation between powder size and sintering rate, B-type of smaller nano-powder is expected to show faster sintering rate than that of relatively larger C-type powder. However, the sintering rate of C-type powder (polygonal shape) was observed to be faster than that of the B-type (sphere shape). Faster sintering behavior of C-type powder can be explained in terms of polygonal morphology of the powder, which makes close contact between powders in compacted specimen. Closely compacted polygonal-shaped powders can accelerate sintering rate due to shorter diffusion distance. In Fig. 4, slight decrease in relative density after full sintering at 1450 °C was observed. The similar trend was also observed by Gupta et al. and attributed to microcracks formed during cooling of fully sintered specimen [9]. Fig. 5 represents the shrinkage rate of the CIPed compacts with sintering temperature. The shrinkage during the sintering of CIPed compacts took place by around 11.5%~12.5%.

Fig. 6 is the scanning electron micrographs showing grain structure of the sintered blocks at various temperatures. As quantitatively shown in Fig. 7, the average grain size increased with a sintering temperature regardless of powder type, and the grain growth seems to be rapid after full densification above 1350 °C. After full densification, almost no difference in grain size was observed among powder types.

Fig. 8 shows the X-ray diffraction patterns of as-received powder and sintered block of three types of

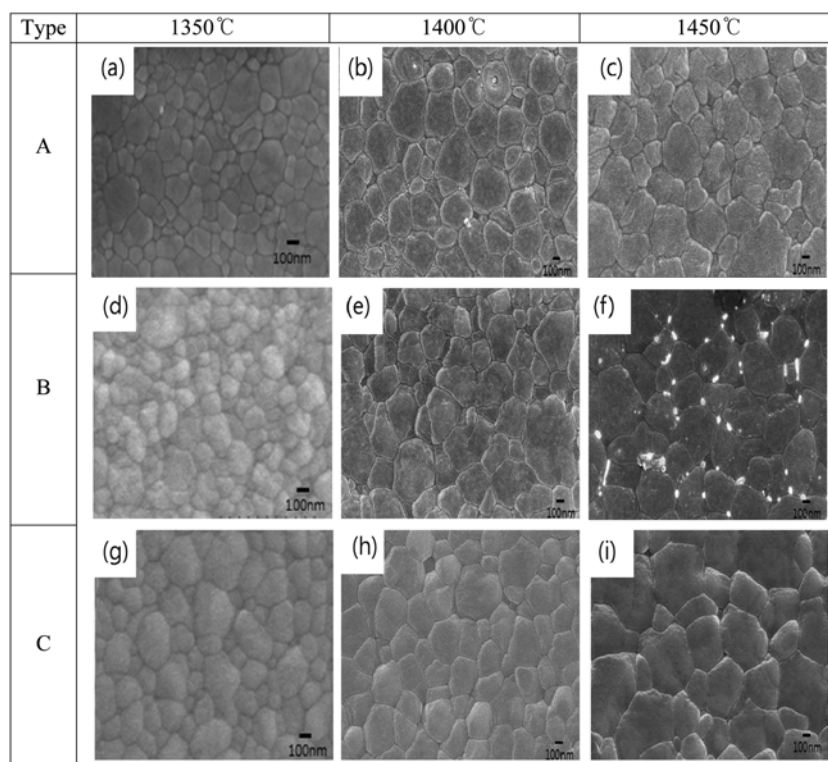


**Fig. 6.** SEM images of the sintered blocks fabricated using different types of powder at various sintering temperature; (a) A-1350 °C, (b) A-1400 °C, (c) A-1450 °C, (d) B-1350 °C, (e) B-1400 °C, (f) B-1450 °C, (g) C-1350 °C, (h) C-1400 °C, (i) C-1450 °C.



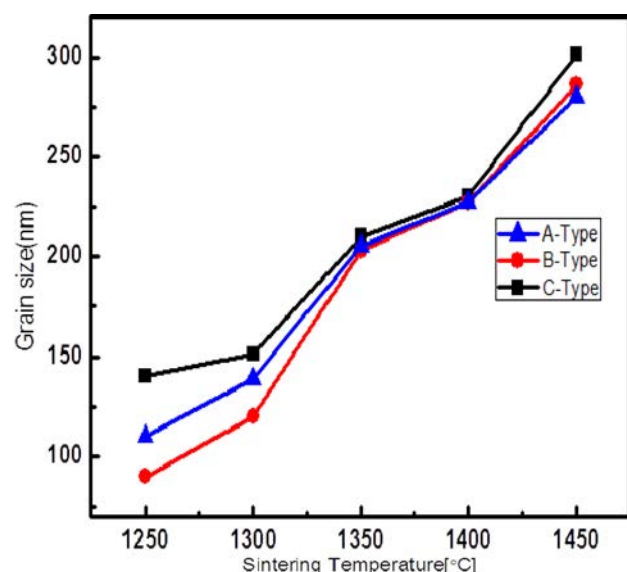


Fig. 7. Change of average grain size with sintering temperature.

commercial powder. For A-type, monoclinic-ZrO<sub>2</sub> phase of about 46% in the as-received powder was fully transformed into tetragonal-ZrO<sub>2</sub> phase after sintering above 1400 °C. For B and C-type, relatively small amount (i.e., 23%) of monoclinic-ZrO<sub>2</sub> existed in the as-received powder, and sintered block of only tetragonal-ZrO<sub>2</sub> phase was obtained after sintering at relatively low temperature of 1350 °C.

For statistical evaluation of the fracture strength based on failure probability, Weibull analysis was performed with 30 biaxial strength data for each type of powder as shown in Fig. 9. From the Y-axis intercept and slop in the graph, scale factor (i.e., probabilistic fracture strength) and shape factor (i.e., Weibull modulus) was determined, respectively. As shown in Fig. 10, the probabilistic fracture strength of A, B and C-type specimen was determined as 630 MPa, 870 MPa, and 920 MPa, respectively. There was difference of about 32% in fracture strength depending on the type of commercial powder, even though almost no difference in chemical composition existed among them. The lowest fracture strength of A-type specimen is inferred to be due to micro-pores existing even after full sintering, considering that the relative density of the sintered specimen is about 98% (Fig. 4). This relatively low density of A-type sintered specimen was already discussed in relation with low compressibility.

The shape factor (i.e., Weibull modulus) was determined as 1.8, 1.8, and 5.5 for A, B, and C-type specimen, respectively. The high shape factor (i.e., steep slope in Weibull regression plot) means that distribution of fracture strength value is narrow. The shape factor of 5.5 is very high value considering that the value of other brittle ceramic material is usually below 3. The highest shape factor of specimen C-type (i.e., 5.5) implies that it is the most reliable and predictable in terms of a fracture behavior of sintered

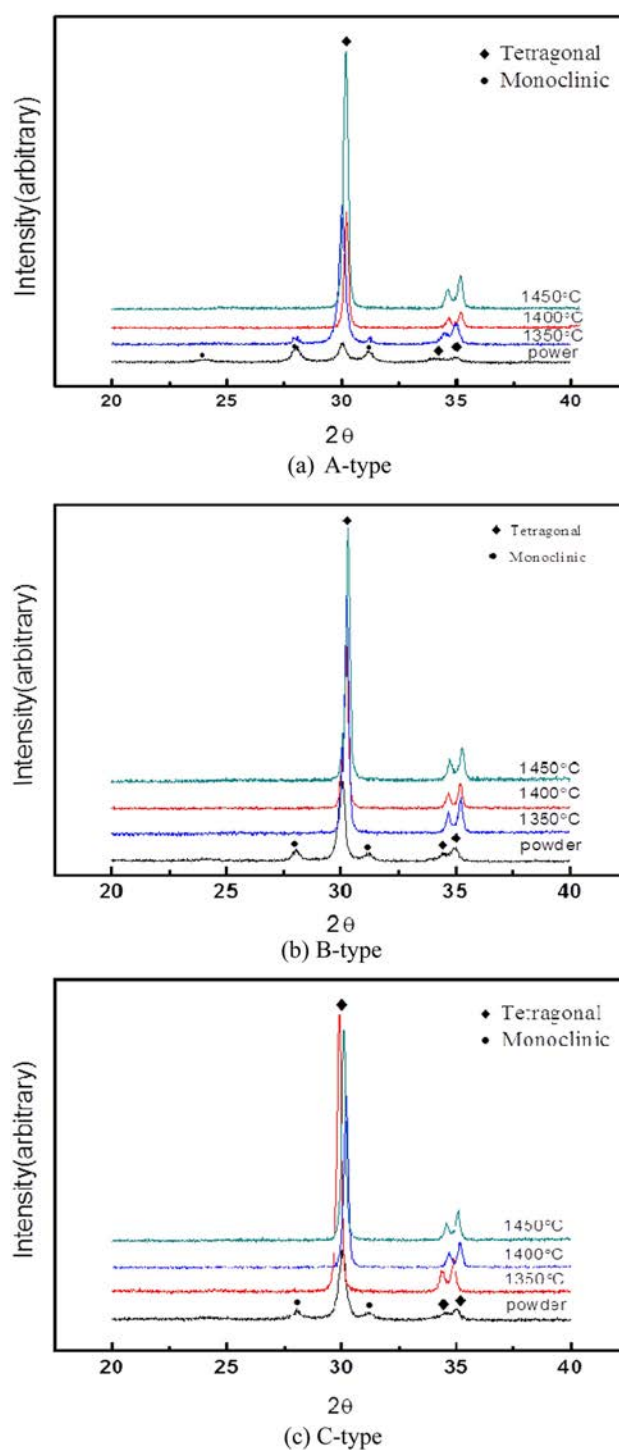


Fig. 8. X-ray diffraction patterns of the as-received powder and sintered block for three types of powder.

3Y-TZP block. On the other hand, the regression slope of A-type specimen seems to change in the Weibull plot shown in Fig. 9. This behavior needs to be further studied in relation with the change in fracture mechanism.

The indentation fracture toughness of fully sintered block was in the range of 5.2–6.7 MPa·m<sup>1/2</sup> for three types of powder, which is similar values with previously reported ones for 3Y-TZP [10]. The well known stress-

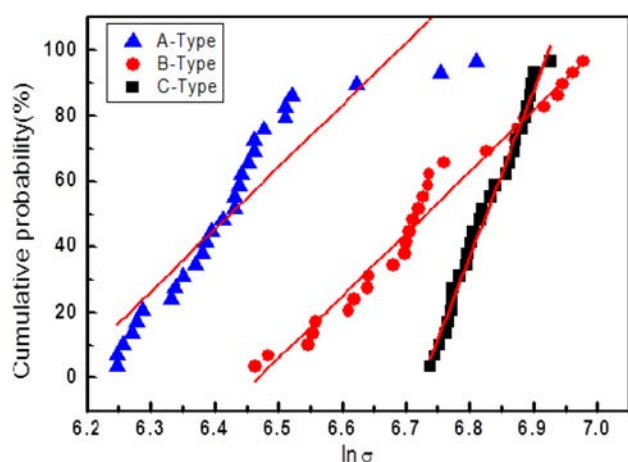


Fig. 9. Weibull plot for determining shape factor (i.e., Weibull modulus) and scale factor.

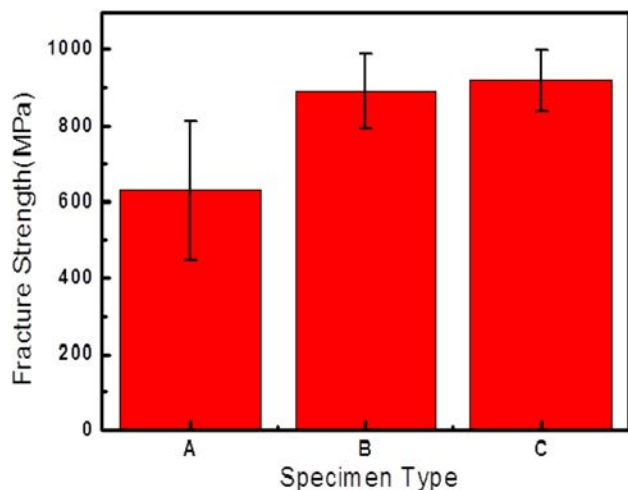


Fig. 10. Comparative value of biaxial strength of the sintered specimens using different types of starting powder.

induced tetragonal-to-monoclinic phase transformation mechanism explains this high fracture toughness of 3Y-TZP ceramics [1, 2, 11].

### Conclusion

The effects of powder characteristics on the sintering

behavior and mechanical properties of dental 3Y-TZP were investigated. Selection of starting spray-dried powder with optimum binding strength between each nano-powder is important to fabricate fully sintered block at relatively low temperature. Based on statistical Weibull regression analysis, shape factor and probabilistic fracture strength were compared among types of powder. About 32% difference in the fracture strength was observed depending on the type of commercial powder, even though almost no difference in chemical composition exists. Powder of polygonal morphology shows the fastest sintering behavior, high strength, and high Weibull modulus of 5.5 implying that it has the most reliable and predictable nature in fracture behavior of sintered 3Y-TZP block. Maximum fracture toughness of  $6.7 \text{ MPa}\cdot\text{m}^{1/2}$  for optimally sintered block is obtained. Under the consideration of micro-pore (i.e., full sintering), grain size (i.e., 200 nm~300 nm), and crystalline phase (i.e., tetragonal), an optimum process condition was established for hybrid manufacturing of personally-fitting CAD/CAM dental block with high strength, high fracture toughness, and high reliability.

### Acknowledgement

This research was supported by Basic Science Research Program through the National Research Foundation of Korea (NRF) funded by the Ministry of Education, Science and Technology(12012012603).

### References

1. C. Piconi, G. Maccauro, *Biomater.* 20 (1999) 1.
2. J. Luo, S. Sadka, R. Stevens, *Mater. Sci.* 33 (1998) 5301.
3. J.A. Mun, E. Jime, *Acta Mater.* 59 (2011) 6670.
4. M. Mazahenri, *J. Euro.Ceram. Soc.* 28 (2008) 2933.
5. R. Dolores, R. Lazar, *Dent. Mater.* 24 (2008) 1676.
6. J. Paul, B. Majeed, K.M. Razeed, J. Barton, *Acta Mater.* 54 (2006) 3991.
7. H. Yillmaz, C. Aydin, *Prosthetic Dentistry* 98 (2007) 120.
8. D.J. Niek, D.K. Marcel, *Dent. Mater.* 22 (2006) 234.
9. T.K. Gupta, *Sci. of Sinter.* 10 (1978) 205.
10. H. Schubert, *J. Amer. Ceram. Soc.* 69 (1986) 270.
11. S.K. Yang, K.M. Bae, B.R. Cho, J.B. Kang, *J. Kor. Ceram. Soc.* 42 (2005) 417.